Marquette University

e-Publications@Marquette

6-2000

Reversible Carbon Monoxide Binding and Inhibition at the Active Site of the Fe-Only Hydrogenase

Brian Bennett
Marquette University, brian.bennett@marquette.edu

Brian J. Lemon
Utah State University

John W. Peters
Utah State University

Follow this and additional works at: https://epublications.marquette.edu/physics_fac

Part of the Physics Commons

Reversible Carbon Monoxide Binding and Inhibition at the Active Site of the Fe-Only Hydrogenase

Brian Bennett
CCLRC Daresbury Laboratory, Warrington WA4 4AD, U.K.
Brian J. Lemon
Department of Chemistry and Biochemistry, Utah State University, Logan, Utah
John W. Peters
Department of Chemistry and Biochemistry, Utah State University, Logan, Utah

SUBJECTS:
Oxides, Peptides and proteins

Abstract

Carbon monoxide binding and inhibition have been investigated by electron paramagnetic resonance (EPR) spectroscopy in solution and in crystals of structurally described states of the Fe-only hydrogenase (CpI) from *Clostridiumpasteurianum*. Simulation of the EPR spectrum of the as-isolated state indicates that the main component of the EPR spectrum consists of the oxidized state of the "H cluster" and components due to reduced accessory FeS clusters. Addition of carbon monoxide to CpI in the presence of dithionite results in the inhibition of hydrogen evolution activity, and a characteristic axial EPR signal [$g_{eff(1)}$, $g_{eff(2)}$, and $g_{eff(3)}$ = 2.0725, 2.0061, and 2.0061, respectively] was observed. Hydrogen evolution activity was restored by successive sparging with hydrogen and argon and resulted in samples that exhibited the native oxidized EPR signature that could be converted to the reduced form upon addition of sodium dithionite and hydrogen. To examine the relationship between the spectroscopically defined states of CpI and those observed structurally by X-ray crystallography, we have examined the CpI crystals using EPR spectroscopy. EPR spectra of the crystals in the CO-bound state exhibit the previously described axial signal associated with CO binding. The results indicate that the addition of carbon monoxide to CpI results in a single reversible carbon monoxide-bound species characterized by loss of enzyme activity and the distinctive axial EPR signal.

Metal-containing hydrogenases occur mainly in prokaryotic organisms and catalyze the reversible conversion of molecular hydrogen to protons and electrons. These enzymes function in fermentative microorganisms to regenerate oxidized electron carriers, and this is coupled to the utilization of molecular hydrogen as a source of reducing equivalents in the hydrogen oxidizing bacteria (*1, 2*). The metal-containing hydrogenases include those that contain both Ni and Fe and those that contain Fe only. Of these two forms, the NiFe hydrogenases are most often associated with hydrogen oxidation, whereas the Fe-only enzymes are most often associated with proton reduction (*1, 2*). Fourier transform infrared (FT-IR) spectroscopic studies have indicated that the active site metal-containing prosthetic groups of both classes of hydrogenases are uniquely organometallic with both metal carbonyl and metal cyanide constituents (*3–5*). Additionally, the structures of both classes have been determined by X-ray crystallography, revealing a unique architecture and offering insights into potential mechanisms of reversible hydrogen oxidation catalyzed by these enzymes (*6–9*).

The structure of the *Clostridiumpasteurianum* Fe-only hydrogenase (CpI) has been determined by X-ray diffraction methods. CpI contains 20 Fe atoms arranged into five [Fe-S] clusters. These clusters include the enzyme active site cluster or "H cluster" and four additional [Fe-S] clusters that presumably participate in electron transfer between external electron donors and acceptors and the active site. The active site cluster comprises a regular [4Fe-4S] cubane bridged to a novel two-Fe cluster through a common cysteine sulfur (Figure 1). The two-Fe cluster is coordinated by, in addition to the cysteine sulfur, two additional sulfur atoms, five diatomic ligands (both carbon monoxide and cyanide), and a terminally bound water molecule (*8*). The assignment of carbon monoxide and cyanide as ligands to the active site Fe atoms is based on the results of FT-IR spectroscopic studies (*3, 4*).
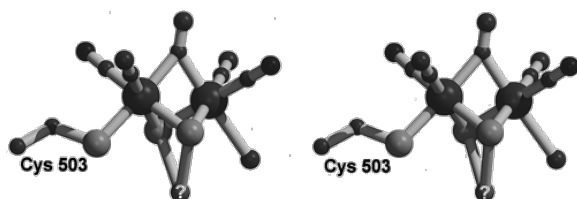

Figure 1 Wall-eyed stereoview of the two-Fe subcluster of the CpI H cluster. Gray scale model with Fe atoms represented as the largest dark gray atoms, S atoms intermediate in size and lighter gray, oxygen atoms smaller

and lightest in color, and carbon atoms black and smallest in size. The S bridging moiety of unknown composition is indicated by a question mark.

The inhibition of the bidirectional Fe-only hydrogenase (CpI) has been studied extensively, and the results have been used to support proposals regarding the mechanism of the enzyme (*10–13*). The first reports concerning carbon monoxide inhibition suggested that inhibition of hydrogen oxidation by carbon monoxide occurred in a competitive manner (*10, 11*). Furthermore, the observed inhibition could be reversed by subsequent photoactivation (*10*). More recently, however, the results of EPR studies have been interpreted to indicate that carbon monoxide binding at the active site occurs sequentially in both noninhibitory and inhibitory modes with inhibition occurring in a manner that was irreversible (*12*). Thus, photoactivation of carbon monoxide-treated enzyme was reinterpreted as being due to the removal of a molecule of carbon monoxide that was bound at the active site but not inhibitory (*13*).

The structure of CpI with exogenously added carbon monoxide bound at the active site has been determined, revealing that a single molecule of carbon monoxide was bound to the active site "H cluster" at a site previously suggested as a possible site of Fe hydride and subsequent hydrogen formation (*14*). In these studies, binding of this single molecule of carbon monoxide resulted in the apparent complete inhibition of the enzyme. This result could therefore not be explained in light of the previous observations suggesting that during carbon monoxide inhibition two molecules of exogenously added carbon monoxide are bound at the active site (*1, 12*). At this point, a complete spectroscopic analysis of the protein crystals had not been performed and a scenario in which the previously characterized native (as crystallized) CpI had already serendipitously bound a single molecule of carbon monoxide could not be ruled out.

Uncertainties have arisen from the apparent differences between the earlier work, describing the effects of carbon monoxide and inhibition, and the more recent work, describing the X-ray crystallographic structure of the apparent carbon monoxide-inhibited form. In the study presented here, carbon monoxide binding and inhibition of CpI have been revisited by detailed EPR spectroscopic examination of CpI in solution and in the crystalline state.

Materials and Methods

EnzymePreparation.

The Fe-only hydrogenase (CpI) from *C.pasteurianum* was purified as described previously (*15, 16*). The carbon monoxide-inhibited form of the enzyme was generated by adding carbon monoxide (UHP grade 99.99%, Matheson) to a 40.5 kPa (0.4 atm) partial pressure of CO with a balance of Ar in a sealed serum vial containing CpI at a concentration of 52 mg/mL in the presence of 2 mM sodium dithionite followed by incubation at room temperature for 5 min. Inhibition was assessed in these samples by monitoring hydrogen evolution upon the addition of carbon monoxide in the bulk protein samples prepared for spectroscopic analysis. Hydrogen evolution activity was determined by assessing hydrogen formation with methyl viologen present as the electron carrier and sodium dithionite present as the electron donor as previously described (*16*). Crystallization of the native and carbon monoxide-inhibited forms of the enzyme was accomplished using the microcapillary batch diffusion method as described previously (*14*). For EPR investigations, 250 μL samples of 0.5 mM CpI in 50 mM Tris buffer (pH 7.4) containing 200 mM KCl were used except where stated. "Oxidized" CpI was prepared by anaerobic direct addition of 3,7-diamino-5-phenothiazinium (thionin, >85%; Sigma) to a final concentration of 0.6 mM (*12*). "Reduced" CpI was prepared by anaerobic direct addition of sodium dithionite to a final concentration of 5 mM (*12*). Incubation of samples with either CO or H_2 was effected by agitating samples under a 9 mL headspace of the relevant gas at a pressure of 40.5 kPa (0.4 atm) with a balance of Ar at 23 °C in sealed vials (Wheaton). Samples were transferred into EPR tubes under Ar and frozen immediately in liquid nitrogen.

When crystalline samples were studied, about 20 crystals were carefully washed in a mother liquor of 100 mM sodium acetate (pH 4.6) containing 25% w/v poly(ethylene glycol) 4000 and 200 mM ammonium acetate and resuspended in 50 μL of the same liquor prior to anaerobic transfer to quartz EPR tubes (Wilmad) and immediate freezing in liquid nitrogen.

EPRSpectroscopy.

EPR spectra were recorded on a Bruker ESP 300E spectrometer equipped with an Oxford Instruments ESR-900 helium flow cryostat and an ER 4116 DM dual mode X-band cavity operating at 9.64–9.65 GHz. Precise microwave frequencies were recorded for each spectrum, and all spectra are presented aligned with a magnetic field range corresponding to a microwave frequency of 9.648000 GHz. A magnetic field modulation frequency of 100 kHz was employed throughout. Other EPR operating parameters are specified in the figure legends. Residual signals due to cavity impurities were removed as in earlier work ([17]–[19]). EPR simulations were performed as described previously ([20]). Where spectra were due to more than one signal, as indicated by simulation, relative amounts of the contributing signals were estimated by double integration of simulations of the individual components. Overall spin quantitation of experimental spectra was performed by comparing integrations with a 2 mM Cu^{2+}−EDTA standard with corrections applied for transition probabilities, temperature, and microwave power as described elsewhere ([21]). For estimation of the "CO-treated" signal, correction factors for temperature dependence were estimated from the data of Adams ([12]).

Results and Discussion

OxidizedCpI.

Oxidized CpI exhibited a characteristic rhombic EPR signal due to a single paramagnetic species (Figure 2a). The signal is due to the oxidized H cluster which exhibits an $S = {}^1/_2$ paramagnetic ground state, and simulation of this species (Figure 2b) provided the EPR parameters $g_{eff(1)}$, $g_{eff(2)}$, and $g_{eff(3)}$ = 2.0973, 2.0392, and 1.9993, respectively, in good agreement with the previously reported g values for this signal ([12]). Upon addition of CO, the rhombic signal was replaced by an axial signal, shown as Figure 2c, which was simulated (Figure 2d) assuming $g_{eff(1)}$, $g_{eff(2)}$, and $g_{eff(3)}$ = 2.0725, 2.0061, and 2.0061, respectively. This species was then flushed with argon for 15 and 60 min, and the EPR spectra were recorded and shown as traces e and g of Figure 2, respectively. Simulation of the spectrum exhibited by the sample after flushing with Ar for 15 min (Figure 2f) indicated that the spectrum consists of a 96% contribution due to the signal from the oxidized enzyme and only a 4% contribution due to the "CO species". After 60 min, the spectrum had reverted entirely to the oxidized species, indicating the binding of CO to oxidized CpI is completely reversible.
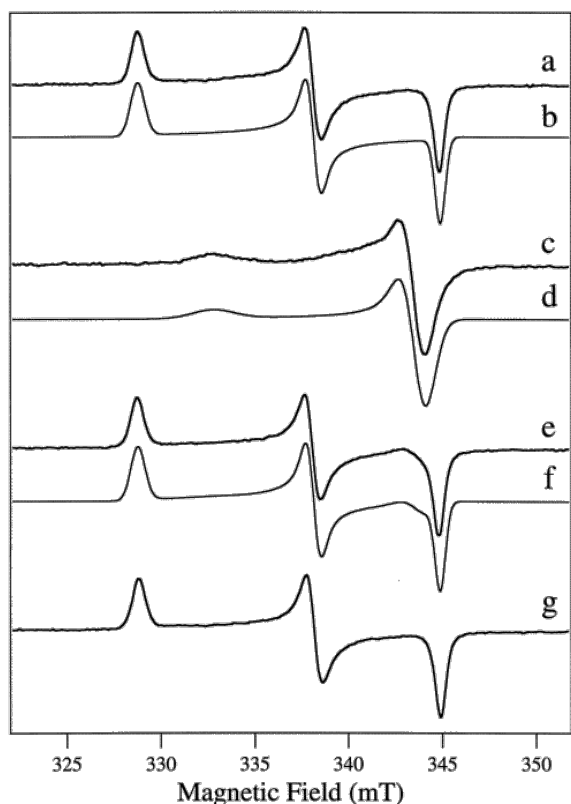
Figure 2 EPR spectra from oxidized and CO-treated CpI. The traces show EPR signals from a single 0.5 mM sample of CpI in 50 mM Tris buffer (pH 7.4) containing 200 mM KCl after sequential treatments as follows: (a) anoxic oxidation with 0.6 mM thionin, (c) anaerobic exposure to 40.5 kPa (0.4 atm) CO for 5 min, (e) anaerobic flushing with Ar for 15 min, and (g) anaerobic flushing with Ar for 60 min. Traces b, d, and f are computer simulations of traces a, c, and g, respectively, assuming for trace a, $g_{eff(1)}$, $g_{eff(2)}$, and $g_{eff(3)}$ = 2.0973, 2.0392, and 1.9993, respectively; for trace d, $g_{eff(1)}$, $g_{eff(2)}$, and $g_{eff(3)}$ = 2.0725, 2.0061, and 2.0061, respectively; and for trace f, there is a 4.4% contribution from trace d and a 95.6% contribution from trace b. Spectra were recorded at 15 (a, e, and g) and 17 K (c), a microwave power of 2 mW, a modulation amplitude of 0.4 mT, a modulation frequency of 100 kHz, and microwave frequencies of 9.64–9.65 GHz; precise microwave frequencies were recorded, and spectra are presented aligned with a magnetic field range corresponding to a microwave frequency of 9.648000 GHz. Spectra are presented normalized for peak-to-baseline intensities. Fractional contributions to trace f were calculated by double integration of the individual components that were summed to provide the simulation.

As-IsolatedandReducedCpI.

The EPR spectrum of as-isolated CpI at 12 K is presented as Figure 3a and is consistent with the spectra for as-isolated CpI reported in the early 1970s (22). The spectrum is complex and clearly consists of more than one paramagnetic species. The spectrum appears to consist of a number of well-defined, and therefore magnetically isolated, $S = {}^1/_2$ species and of a broader ill-defined signal, perhaps due to magnetically coupled centers. The contribution to the spectrum due to magnetically isolated reduced [Fe-S] clusters could be simulated (Figure 3b) by assuming three species, one of which corresponded to the oxidized H cluster (Figure 3c), a second species with $g_{eff(1)}$, $g_{eff(2)}$, and $g_{eff(3)}$ = 2.0802, 2.0032, and 1.9795, respectively (Figure 3d), and a third species with $g_{eff(1)}$, $g_{eff(2)}$, and $g_{eff(3)}$ = 2.0880, 2.0175, and 2.0048, respectively (Figure 3e). These assignments are, as of yet, tentative, and further detailed characterization of the relaxation properties of these signals is in progress to facilitate unambiguous characterization of the signals and assignment to specific crystallographically identified [Fe-S] clusters. Careful examination of the broad underlying feature in the spectrum revealed a close similarity to the spectrum of dithionite-reduced CpI (Figure 3f). This spectrum is ill-defined and very broad and is

characteristic of extensively spin-coupled multiple iron–sulfur clusters. Inclusion of a proportion of this signal corresponding to 0.9 spin mol^{-1} further improved the simulation (Figure 3g) of the experimental spectrum.
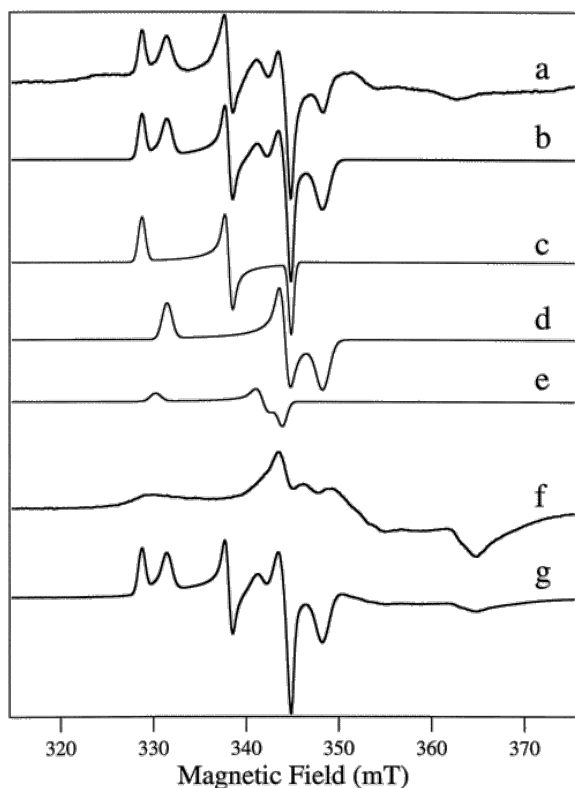

Figure 3 EPR signal from as-prepared CpI. Trace a shows the EPR signal from as-prepared CpI in 50 mM Tris buffer (pH 7.4) containing 200 mM KCl. Trace b is a computer simulation of trace a assuming three distinct isolated species (c–e), with fractional contributions of (c) 38.0%, (d) 51.4%, and (e) 10.6%. Traces c–e are the individual simulations assuming for trace c, $g_{eff(1)}$, $g_{eff(2)}$, and $g_{eff(3)}$ = 2.0973, 2.0392, and 1.9993, respectively; for trace d, $g_{eff(1)}$, $g_{eff(2)}$, and $g_{eff(3)}$ = 2.0802, 2.0032, and 1.9795, respectively; and for trace e, $g_{eff(1)}$, $g_{eff(2)}$, and $g_{eff(3)}$ = 2.0880, 2.0175, and 2.0048, respectively. Trace f is the EPR signal from CpI reduced with 5 mM sodium dithionite. Trace g is an alternative simulation of trace a obtained by summing a 44.6% contribution of trace b and a 55.4% contribution of trace f. Experimental spectra were recorded at 15 K, a microwave power of 1 mW, a modulation amplitude of 0.4 mT (a) or 1.0 mT (f), a modulation frequency of 100 kHz, and microwave frequencies of 9.64–9.65 GHz; precise microwave frequencies were recorded, and spectra are presented aligned with a magnetic field range corresponding to a microwave frequency of 9.648000 GHz. Spectra are presented with arbitrary intensities. Fractional contributions to traces b and g were calculated by double integration of the individual components which were summed to provide the simulation.

CpI was reduced from the as-isolated state with 10 equiv of sodium dithionite, and the EPR spectrum is presented as Figure 4c. Upon incubation of reduced CpI under CO, hydrogen evolution activity was undetectable and a new complex signal was observed (Figure 4d). This complex signal integrated to about 2 spins mol^{-1} and is composed of about 50% of the CO spectrum observed upon incubation of oxidized CpI with CO (cf. traces c and d of Figure 2) and 50% of a complex, poorly resolved spectrum. The appearance of the CO signal was clearly unrelated to adventitious oxidation of the enzyme by O_2; not only were all experiments carried out strictly anaerobically, but the reduced enzyme was also maintained in the presence of sodium dithionite. Furthermore, at no stage was a signal indicative of O_2 binding to the H cluster observed (1, 13). The broader signal upon which the CO signal is superimposed was intermediate in appearance between that of the as-prepared enzyme and the dithionite-reduced enzyme. The outermost features of the signal were broad and asymmetric, exhibiting line

shapes that are analogous to the outer lines of the reduced signal. However, these lines are shifted toward the center of the signal relative to the reduced signal; the low-field line has moved from 329.8 to 332.9 mT, and the high-field line has moved from 364.8 to 358.6 mT.
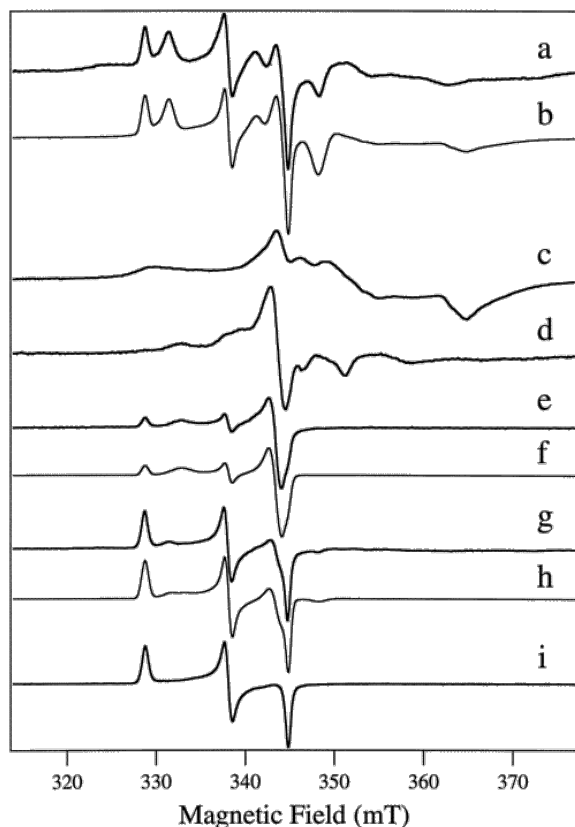

Figure 4 EPR signals from as-prepared, reduced, and CO-treated CpI. Trace a shows the spectrum of as-prepared CpI in 50 mM Tris buffer (pH 7.4) containing 200 mM KCl (cf. Figure 3a). Trace b is the simulation of trace a shown as Figure 3g, generated as described in the legend of Figure 3. Traces c–e, g, and i are EPR spectra of CpI upon (c) reduction with hydrogen in the presence of sodium dithionite, and subsequent exposure to 0.4 atm CO for 5 min, (d) followed by flushing anaerobically with Ar for 5 min, (e) addition of H_2 and dithionite and incubation for 3 min followed by flushing with Ar for additional 5 min, (g) and again incubation with H_2 and 1 mM dithionite for 3 min followed by flushing with Ar for an additional 5 min (i). Traces f and h are simulations assuming mixtures of the simulations of "oxidized" and "CO-treated" CpI shown as traces b and d of Figure 2, respectively. Trace f assumes 0.29 spin mol^{-1} of the oxidized CpI species and 0.71 spin mol^{-1} of the CO-treated species; trace h assumes 0.79 and 0.21 spin mol^{-1} of the oxidized and CO-treated species, respectively, and a 0.05 spin mol^{-1} contribution from signal A. Spectra were recorded at 15 K, a microwave power of 2 mW, a modulation amplitude of 0.4 (a, d, e, g, and i) or 1.0 mT (c), a modulation frequency of 100 kHz, and microwave frequencies of 9.64–9.65 GHz; precise microwave frequencies were recorded, and spectra are presented aligned with a magnetic field range corresponding to a microwave frequency of 9.648000 GHz. Spectra are presented with arbitrary intensities. Fractional contributions to traces b, f, and h were calculated by double integration of the individual components that were summed to provide the simulations.

Other features in the spectrum of reduced CpI upon short exposure to CO (Figure 4d) include resolved lines at 346.6 and 351.2 mT, which may or may not be related to the lines in the reduced spectrum at 344 and 348 mT, and a poorly resolved feature centered at 340 mT. The resolution of lines in the spectrum of CO-treated reduced CpI and, particularly, the movement of the high- and low-field lines toward the center of the spectrum are indicative of a dimunition of the spin coupling observed for the iron–sulfur clusters. The most likely explanation

for this is that one of the clusters has become oxidized and the overall magnetic interaction experienced by each of the other clusters is reduced. A very similar phenomenon has been described for the iron−sulfur clusters of *Escherichiacoli* membrane-bound respiratory nitrate reductases A and Z. *E.coli* nitrate reductase contains three $[4Fe-4S]^{2+/1+}$ and one $[3Fe-4S]^{1+/0}$ cluster and is comparable to CpI in terms of its complement of paramagnetic centers in the oxidized and reduced forms (*23−25*). Upon reduction of the [3Fe-4S] cluster and one [4Fe-4S] cluster, no magnetic coupling is indicated by the EPR spectrum, though the $[3Fe-4S]^0$ cluster is likely in the $S = 2$ state. Upon reduction of a second [4Fe-4S] cluster, a degree of magnetic interaction is observed, but upon reduction of the third, low-potential [4Fe-4S] cluster, extensive magnetic interactions are observed and a broad, essentially featureless signal is observed which is not dissimilar to that from reduced CpI.

The EPR spectrum of CO-treated reduced CpI presented in Figure 4d indicates not only oxidation of the H cluster upon formation of the CO-bound species but also partial oxidation of the iron−sulfur complement of the enzyme. This in turn may be indicative of catalysis of slow proton reduction by CpI occurring in the presence of dithionite despite the presence of CO, suggesting that CO is a competitive rather than an irreversible inhibitor. This is consistent with observations concerning specific activity measurements that indicate that activity can be restored if CO is removed from concentrated samples. In addition, when small aliquots of concentrated CO-inhibited CpI are transferred to assay vials that do not contain CO, full activity [3100 nmol of H_2 formed min^{-1} (mg of CpI)$^{-1}$] is observed.

Following incubation of reduced CpI under CO for 5 min, the sample was flushed with Ar gas for 5 min and the EPR signal recorded (Figure 4e). An excellent simulation was obtained (Figure 4f) which assumed 0.18 spin mol^{-1} due to the oxidized signal and 0.82 spin mol^{-1} for the CO species. No signals due to iron−sulfur clusters were detected, indicative of complete oxidation of the iron−sulfur complement. The CpI sample atmosphere was then exchanged with 100% H_2, and 1 mM dithionite was added. After a 3 min incubation period under H_2, the sample was flushed with Ar as before, yielding a spectrum (Figure 4g), of which simulation (Figure 4h) indicated that only 21% of the H clusters in the sample were now in the CO-bound form, with the remainder exhibiting the oxidized signal. The addition of H_2 to the CO-bound and inhibited CpI stimulated the removal of CO, consistent with the previously observed competitive manner of inhibition with respect to hydrogen oxidation (*10, 11*). After an additional cycle of H_2 incubation (3 min) and Ar flushing, the resulting spectrum was completely due to the oxidized H cluster (Figure 4i). Complete removal of CO could be accomplished with samples without addition of H_2 by multiple cycles of Ar flushing over a period of 1 h.

Upon incubation of the reduced CpI with CO, a species is generated that is indistinguishable from the CO-bound H cluster of the oxidized enzyme. CO is not redox active, and therefore, oxidation of both the H cluster and the iron−sulfur clusters can only arise as a consequence of proton reduction by the reduced enzyme. The EPR data indicate that this process can occur slowly in the presence of CO and that CO cannot be an irreversibly binding inhibitor of either the oxidized or reduced enzyme. Irreversible binding of CO to the reduced H cluster would result in an EPR-silent species that would be unable to reduce protons and therefore would remain in the reduced state. However, estimations of the CO signal's contribution to Figure 4e by integration and to Figure 4d by observation of 0.71 and about 1 spin mol^{-1}, respectively, clearly suggest that prior to CO removal most of the H clusters in a frozen sample are trapped in the oxidized CO-bound form. Yet, the lack of an iron−sulfur component in the spectrum of Figure 4e compared to Figure 4d clearly shows that the enzyme is still capable of redox reaction even though the H clusters are largely in the CO-bound form. The only simple scenario consistent with all the data, then, is that CO is a reversible, competitive inhibitor of CpI. It is entirely possible that CO does not bind the reduced H cluster of CpI at all or else is highly labile. Indeed, demonstration of CO binding to the reduced cluster would be very difficult. The putative CO-bound reduced H cluster would likely be EPR-spectroscopically silent. The reduced H cluster in the presence of CO is unstable in that it reverts to the oxidized CO-bound form, presumably due to slow turnover, so radioactive tracing with ^{14}CO is not practical. Vibrational

spectroscopic methods would have to be carried out in the frozen state and would be hindered by the presence of Fe−CO moieties in the resting enzyme. Evaluation of the practicability of rapid diffusion of CO into reduced crystals of CpI followed by flash-freezing is ongoing. Regardless, binding of CO to the oxidized cluster clearly does occur, though the Ar flushing experiments suggest a bulk time constant for dissociation of CO of around 2−7 min, depending on precise conditions.

CrystallineCpI.

The data from solution studies with CpI clearly indicate that CO binds reversibly to the enzyme, yielding a single, characteristic EPR-detectable species of the H cluster. Structural characterization of the CO-inhibited form of CpI (*14*) indicated that, in addition to the ligands to the terminal iron atom found in the native CpI structure, Fe2 (Figure 1), electron density consistent with the presence of an additional single CO molecule bound to Fe2. However, reports in the literature (*13*) have suggested that the EPR signal is, in fact, due to binding of a CO molecule that is not inhibitory. In the complex scenario previously proposed, both a noninhibitory CO molecule and a second irreversibly binding inhibitory molecule will react with the enzyme under conditions of enzyme turnover. We therefore wished to investigate whether the crystallographically characterized CpI species, in which only one molecule of exogenous CO is observed bound, corresponded to the CO species observed by EPR.

An EPR spectrum of crystals of as-isolated CpI is presented as Figure 5a. The spectrum contained features also present in the spectrum of as-isolated CpI in solution (cf. Figure 5b). Features identifiable as being due to the oxidized signal were observed at 329 and 337 mT, and a split feature was observed at 344 mT. Some of these features were shifted slightly from the corresponding positions in the spectrum of the enzyme in frozen solution. Indeed, the spectrum exhibited some sensitivity to the orientation of the sample in the spectrometer and the precise positions of the features shifted around the positions observed in the solution spectra as a function of sample orientation. Approximately 20 crystals were washed and suspended in synthetic mother liquor prior to transfer to an EPR tube, and it is likely that 10−15 crystals were in the frozen drop that was positioned between the cavity and the modulation coils. Therefore, a true "powder spectrum" could not be obtained, and the observed spectrum represents the sum of 10−15 single-crystal spectra, each of which has resonance positions dependent upon the precise orientation of the crystal. Nevertheless, the approximation to a powder spectrum is sufficient to allow identification of the oxidized H cluster signal.
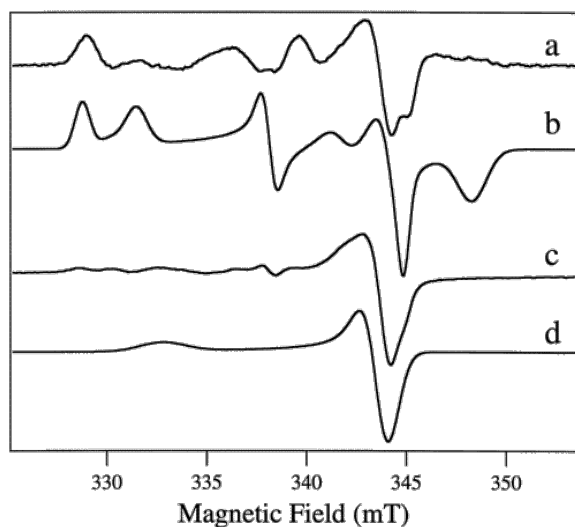

Figure 5 EPR signals from crystalline CpI. EPR spectra are presented of crystals of (a) as-prepared and (c) CO-treated CpI, in 100 mM sodium acetate (pH 4.6) containing 25% w/v poly(ethylene glycol) 4000 and 200 mM ammonium acetate. About 20 crystals were maintained in suspension in crystallization mother liquor and frozen rapidly prior to EPR spectroscopic investigation. For comparison, simulations of frozen solution spectra of as-prepared and CO-treated CpI in 50 mM Tris buffer (pH 7.4) containing 200 mM KCl are shown as traces b and d,

respectively (also shown and described as Figures 3b and 2d). Experimental spectra were recorded at 15 (a) and 12 K (c), a microwave power of 2 mW, a modulation amplitude of 0.4 mT, and a modulation frequency of 100 kHz and are presented aligned with a magnetic field range corresponding to a microwave frequency of 9.648000 GHz.

EPR analysis of crystals of the CO bound state of CpI yielded a spectrum (Figure 5c) that is almost entirely (>95%) due to a CO signal that is indistinguishable from that observed in frozen solution. Therefore, it can be concluded that the species characterized by EPR and that characterized by crystallography are the same and that the crystallographically characterized species corresponds to an inhibited species of CpI containing a single molecule of CO reversibly bound to the H cluster.

Acknowledgment

References

1 Adams, M. W. W. (1990) *Biochim.Biophys.Acta1020*, 115−45.
2 Przybyla, A. E., Robbins, J., Menon, N., and Peck, H. D., Jr. (1992) *FEMSMicrobiol. Rev.8*, 109−35.
3 Happe, R. P., Roseboom, W., Pierik, A. J., Albracht, S. P., and Bagley, K. A. (1997) *Nature385*, 126.
4 Pierik, A. J., Hulstein, M., Hagen, W. R., and Albracht, S. P. (1998) *Eur. J.Biochem. 258*, 572−8.
5 van der Spek, T. M., Arendsen, A. F., Happe, R. P., Yun, S., Bagley, K. A., Stufkens, D. J., Hagen, W. R., and Albracht, S. P. (1996) *Eur. J.Biochem.237*, 629−34.
6 Volbeda, A., Charon, M. H., Piras, C., Hatchikian, E. C., Frey, M., and Fontecilla-Camps, J. C. (1995) *Nature373*, 580−7.
7 Higuchi, Y., Yagi, T., and Yasuoka, N. (1997) *Structure5*, 1671−80.
8 Peters, J. W., Lanzilotta, W. N., Lemon, B. J., and Seefeldt, L. C. (1998) *Science282*, 1853−8.
9 Nicolet, Y., Piras, C., Legrand, P., Hatchikian, C. E., and Fontecilla-Camps, J. C. (1999) *Structure7*, 13−23.
10 Thauer, R. K., Kaufer, B., Zahringer, M., and Jungermann, K. (1974) *Eur.J.Biochem. 42*, 447−52.
11 Erbes, D. L., and Burris, R. H. (1978) *Biochim. Biophys.Acta525*, 45−54.
12 Adams, M. W. (1987) *J.Biol.Chem.262*, 15054−61.
13 Kowal, A. T., Adams, M. W., and Johnson, M. K. (1989) *J.Biol.Chem.264*, 4342−8.
14 Lemon, B. J., and Peters, J. W. (1999) *Biochemistry38*, 12969−73.
15 Chen, J. S., and Mortenson, L. E. (1974) *Biochim.Biophys.Acta371*, 283−98.
16 Adams, M. W. W., and Mortenson, L. E. (1984) *Biochim. Biophys.Acta766*, 51−61.
17 Bennett, B., and Holz, R. C. (1997) *Biochemistry36*, 9837−46.
18 Bennett, B., and Holz, R. C. (1998) *J.Am.Chem.Soc.120*, 1923−33.
19 Bennett, B., and Holz, R. C. (1998) *J.Am.Chem.Soc.120*, 12139−40.
20 Butler, C. S., Charnock, J. M., Bennett, B., Sears, H. J., Reilly, A. J., Ferguson, S. J., Garner, C. D., Lowe, D. J., Thomson, D. J., Berks, B. C., and Richardson, D. J. (1999) *Biochemistry38*, 9000−12.
21 Barber, M. J., Bray, R. C., Lowe, D. J., and Coughlan, M. P. (1976) *Biochem.J.153*, 297−307.
22 Nakos, G., and Mortenson, L. E. (1971) *Biochemistry10*, 2442−9.
23 Johnson, M. K., Bennett, D. E., Morningstar, J. E., Adams, M. W. W., and Mortenson, L. E. (1985) *J.Am.Chem.Soc.107*, 5456−63.
24 Guigliarelli, B., Asso, M., More, C., Augier, V., Blasco, F., Pommier, J., Giordano, G., and Bertrand, P. (1992) *Eur.J.Biochem.207*, 61−8.
25 Bennett, B., and Bray, R. C. (1994) *Biochem.Soc.Trans.22*, 283.